Colloids and Surfaces B: Biointerfaces 170 (2018) 609–616

Contents lists available at ScienceDirect

Colloids and Surfaces B: Biointerfaces

journal homepage: www.elsevier.com/locate/colsurfb

Soft nanoparticles charge expression within lipid membranes: The case of amino terminated dendrimers in bilayers vesicles

Domenico Lombardo[a,*], Pietro Calandra[b], Salvatore Magazù[c], Ulderico Wanderlingh[c], Davide Barreca[d], Luigi Pasqua[e], Mikhail A. Kiselev[f]

[a] Consiglio Nazionale delle Ricerche, Istituto per i Processi Chimico-Fisici, 98158 Messina, Italy
[b] Consiglio Nazionale delle Ricerche, Istituto Studio Materiali Nanostrutturati, 00015 Roma, Italy
[c] Dipartimento di Fisica e Scienze della Terra, Università di Messina, 98166 Messina, Italy
[d] Dipartimento di Scienze chimiche, biologiche, farmaceutiche ed ambientali, Università di Messina, 98166 Messina, Italy
[e] Department of Environmental and Chemical Engineering, University of Calabria, 87036 Rende (CS), Italy
[f] Frank Laboratory of Neutron Physics, Joint Institute for Nuclear Research, Dubna, Moscow 141980, Russia

ARTICLE INFO

Keywords:
Dendrimers
Bio-membranes
Charged nanoparticles
zeta potential
Raman spectroscopy
Scattering techniques

ABSTRACT

Interactions of charged nanoparticles with model bio-membranes provide important insights about the soft interaction involved and the physico-chemical parameters that influence lipid bilayers stability, thus providing key features of their cytotoxicity effects onto cellular membranes. With this aim, the self-assembly processes between polyamidoamine dendrimers (generation G = 2.0 and G = 4.0) and dipalmitoylphosphatidylcholine (DPPC) lipids were investigated by means of Zeta potential analysis, x-rays, Raman and quasielastic light scattering experiments. Raman scattering data evidenced that dendrimers penetration produce a perturbation of the DPPC vesicles alkyl chains. A linear increase of liposome zeta-potential with increasing PAMAM concentration evidenced that only a fraction of the dendrimers effective charge contributes to the expression of the charge at the surface of the DPPC liposome. The linear region of the zeta-potential extends toward higher PAMAM concentrations as the dendrimer generation decreases from G = 4.0 to G = 2.0. Further increase in PAMAM concentration, outside of the linear region, causes a perturbation of the bilayer characterized by the loss in multilamellar correlation and the increase of DPPC liposome hydrodynamic radius. The findings of our investigation help to rationalize the effect of nanoparticles electrostatic interaction within lipid vesicles as well as to provide important insights about the perturbation of lipid bilayers membrane induced by nanoparticles inclusion.

1. Introduction

Dendrimers are globular hyperbranched polymeric architectures with easily controllable properties which have attracted a great interest as an efficient platform for drug delivery and nanomedicine applications [1–5]. Despite the significant increase in the number of their biological applications reported in last decade, some critical issues still remain which are mainly connected with possible disruptive effect during the interaction with biological membranes and that may be associated with unwanted cytotoxicity effects [6–11].Polymer-based charged nanoparticles, such as dendrimers, and the study of their interactions with model bio-membranes provide important examples for the investigation of the effect of foreign molecules on liposomes structures [12–16]. Nanoparticles inclusion also furnishes important insights about the soft interaction involved in biological systems, thus highlighting the physico-chemical parameters and properties that primarily influence their stability, and provides indication about the key features of cytotoxicity effects onto cellular membranes [17–20]. Finally, charged polymer-based inclusion components can be designed to strongly interact with the lipid structure at different solution conditions, thus furnishing a pathway to design charge-responsive lipid structures for applications in drug delivery [20–22].

Herein we investigate the charge effects of positively charged amine terminated (G = 2.0 and G = 4.0) PAMAM dendrimers on DPPC vesicles, at the temperature of T = 20 °C. As the dendrimer charge is among the main control parameters, the dendrimer's electrostatic interaction has been primarily investigated in order to elucidate the effect of dendrimer inclusion on DPPC lipid bilayers.

* Corresponding author.
E-mail address: lombardo@ipcf.cnr.it (D. Lombardo).

https://doi.org/10.1016/j.colsurfb.2018.06.031
Received 15 February 2018; Received in revised form 12 June 2018; Accepted 17 June 2018
Available online 19 June 2018

2. Materials and methods

2.1. Dendrimers

Generation G = 2.0 (M_w = 3256 g/mol) and G = 4.0 (M_w = 14,215 g/mol) polyamidoamine (PAMAM) dendrimers were purchased from Sigma Aldrich and consist of a tetrafunctional ethylenediamine core with 16 and 64 amine (-NH_2) terminal groups in average respectively. Both dendrimers were used without further purification.

Phospholipid. Synthetic 1,2-dipalmitoyl-sn-glycero-3-phosphocholine (DPPC) (M_w = 734 g/mol) was purchased from Avanti Polar Lipids, and used without further purification.

2.2. Liposome preparation

Various dendrimer-lipid molar fractions X were prepared by adding the methanol solution of the dendrimers to the DPPC lipids, while pure chloroform was added until all of the lipids was dissolved. The mixture was dried under vacuum conditions to evaporate the solvent. The resulting lipid film was hydrated with an appropriate volume of water solution containing 10 mM NaCl salt. Lipid mixtures were incubated above the DPPC lipid phase-transition temperature (T_m = 41 °C). Subsequently (at $T > T_m$) the suspension was forced to pass 20 times through a polycarbonate membrane of 50 nm pore radius, mounted in a mini-extruder (Avanti Polar Lipids) fitted with two 1000-μl Hamilton gastight syringes. The final lipid concentration was 10 mg/ml.

2.3. Raman spectroscopy

Raman scattering measurements of the PAMAM/DPPC system were performed at the temperature of T = 20 °C using a Spectrum GX Perkin Fourier-transform spectrophotometer. The used excitation source was the 514.5 nm line of an Ar laser (Spectra Physics 2020) operating at mean power of 300 mW (which was controlled to be stable during the measurements).

2.4. Zeta (ζ) potential and light scattering measurements

Particle zeta potential experiments were performed by measuring the electrophoretic mobility μE (for particles of sizes > 5 nm) using a Zeta PALS Brookhaven instrument equipped with a diode laser at a power P = 30 mW and wavelength of λ = 661 [23,24]. The same instrument has been used to perform quasi-elastic light scattering (QELS) experiments. In a QELS experiment, the laser scattered intensity-intensity time correlation function, $g^2(t)$, furnishes information of the hydrodynamic radius R_H of diffusing nanoparticles in solution, by analyzing the translational diffusion coefficient $D = K_BT/6\pi\eta R_H$ (where k_B is the Boltzmann constant, T the absolute temperature, and η the viscosity of the solvent) [25]. Both zeta potentials and QELS experiments results were averaged from 5 to 7 measurements.

2.5. Small angle X-ray scattering

Small angle x-rays scattering (SAXS) experiments have been performed by a laboratory instrumentation consisting of a Philips PW X-ray generator with a Kratky type small-angle camera in the finite slit height geometry. Part of the SAXS experiments was also performed at the SWING beamline at the SOLEIL Synchrotron radiation facility in Saint-Aubin (France). The wavelength of the incident X-ray beam were λ = 1.54 Å. The scattered intensity I(q), collected at various scattering angles θ with respect to the incident radiation direction and expressed as a function the scattering wavevector $q = (4\pi/\lambda)\sin(\theta/2)$, was normalized with respect to transmission and corrected by the empty cell and solvent contribution.

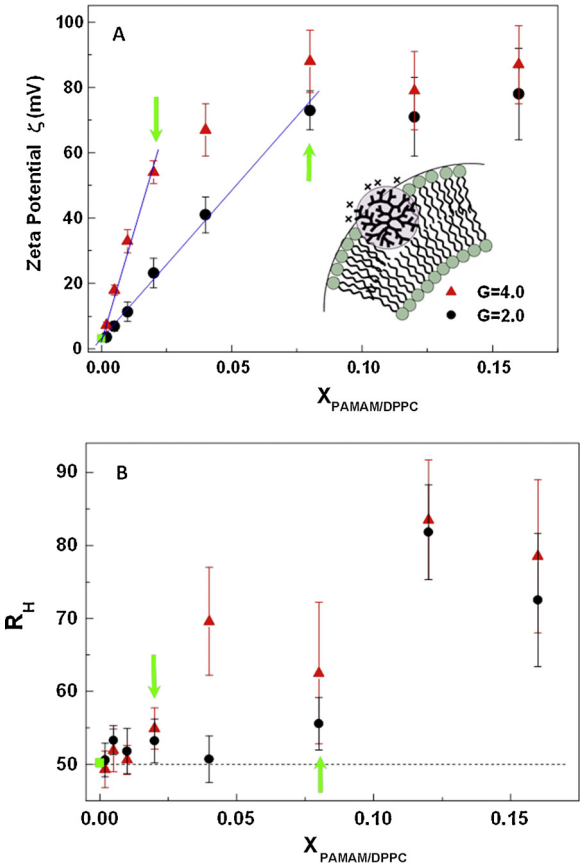

Fig. 1. (A) Zeta potentials (ζ) of the extruded vesicles as a function of the PAMAM-DPPC molar fractions X, for the generation G = 2.0 (black circles) and G = 4.0 (red triangles). (B) Corresponding hydrodynamic radius R_H of the PAMAM/DPPC mixed system. Results for the DPPC vesicles in absence of dendrimers are also reported for comparison (green circle).(For interpretation of the references to colour in this figure legend, the reader is referred to the web version of this article.).

3. Results

3.1. Zeta (ζ) potential and light scattering measurements

The effect of the interaction between the charged PAMAM dendrimers (generation G = 4.0 and G = 2.0) on DPPC liposomes, evaluated in terms of modulation of particles ζ-potential, is reported in Fig. 1A. The addition of the positively charged amine terminated (-NH_2) PAMAM dendrimers causes an increase of the zeta potential of the vesicles as a function of dendrimer concentration from 3.2 mV (in absence of dendrimers) to about 80 mV, at the higher dendrimer concentration.

It is worth pointing out that the initial variation of the ζ-potential is linearly dependent on dendrimer concentrations up to a given concentration X (see arrows in Fig. 1A). Beyond this linear range, the zeta potential was characterized by a slow increase and a higher fluctuation around its average value (higher error bars).

The hydrodynamic radius R_H of liposomes in low concentration region of dendrimers, measured by dynamic light scattering (DLS) experiments (Fig. 1B), indicated the presence of vesicles with an average radius comparable to the extruder (membrane) pore radius (R = 50 nm). The presence of a single decay-time in the intensity-intensity time correlation function $g^2(t)$, indicate the absence of free dendrimers in solution. A significant increase in the size (and size fluctuation) has been detected during the repeated measurements of the liposome mixed system, starting from a given dendrimer concentration

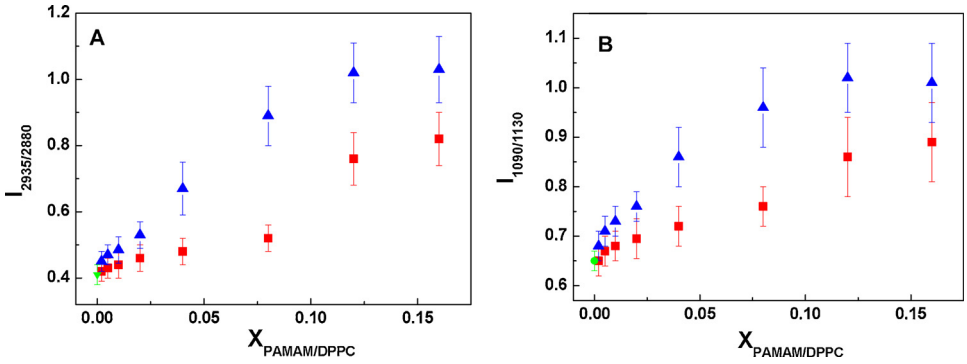

Fig. 2. Raman scattering peak height intensity ratios I(2935/2880) of the extruded vesicles as a function of the PAMAM/DPPC molar fractions X, for the PAMAM dendrimers of generation G = 2.0 (red squares) and G = 4.0 (blue triangles) (A). The corresponding peak height intensity ratios I(1090/1130) is reported in (B). Result obtained for the solely DPPC lipid system is also reported (green symbols) for comparison.(For interpretation of the references to colour in this figure legend, the reader is referred to the web version of this article.).

(corresponding to the non-linear behavior of the ζ-potential). A significant fluctuation in the liposome size and ζ-potential at the higher dendrimer concentration may be connected to the degradation of liposomes structures. The large amount of dendrimers probably creates a considerable degree of discontinuity in compact structure of the DPPC lipid bilayer that causes the disruption of the primary lamellar stacks, followed by the successive formation of larger complex aggregates.

3.2. Raman spectroscopy

Analysis of the Raman spectrum bands allows to detect the structural changes produced by inclusion of PAMAM dendrimers in DPPC lipid membranes structures. More specifically, the height intensity ratio I(2935/2880) between the Fermi resonance band of terminal $-CH_3$ (at 2935 cm^{-1}) and the antisymmetrical vibration (at 2880 cm^{-1}) of lipid alkyl chains can be used as an indicator to describe the main (inter- and intra-chain) changes occurring in the lipids hydrocarbon region and is then sensitive to changes in conformational order from rotations, twists, kinks and bends of the lipid chains (order-disorder transitions) [26,27].

Fig. 2A evidences an increase in the Raman scattering peak height intensity ratios I(2935/2880) with increasing amount of dendrimers for the DPPC/PAMAM (generations G = 2.0 and G = 4.0) systems, thus indicating that inclusion of both typology of dendrimers causes changes in lateral steric hindrance of the hydrocarbon-chain region of the DPPC lipid bilayers. This trend is confirmed by a similar increase of the peak height intensity ratios I(1090/1130) (Fig. 2B) which indicates an increase of the disorder/order ratio of the lipids (alkyl chains) C—C stretching modes [26,27], due to the increase of the peak at 1090 cm^{-1} (gauche conformation) with respect to that at 1130 cm^{-1} (trans conformation). Insertion of the two types of PAMAM dendrimers promotes then an order to disorder transition caused by the perturbation and liquidation of the compact hydrophobic region of the lipid bilayer, which is more effective with the higher generation G = 4.0 dendrimers.

3.3. Small angle X-rays scattering (SAXS) experiments

3.3.1. SAXS characterization of PAMAM dendrimers in water solution

SAXS experiments have been performed with the aim to obtain useful information about structure and inter-dendrimer interaction for the two investigated typologies of dendrimers in water solution. In Fig. 3 the SAXS spectra for the two generation of G = 2.0 and G = 4.0 at two different concentrations are reported. The presence of wide peaks for the most concentrated samples evidences a liquid-like, long range order that can be explained by electrostatic repulsion caused by the (partial) ionization of the dendrimer's surface end-groups ($-NH_3^+$).

Assuming a monodisperse dendrimer system, the SAXS scattering intensity $I(q) = N(\Delta\rho)^2 P(q)S(q)$ is expressed in terms of the product of the form factor P(q) and the structure factor S(q) [28], where N is the particles number density, while $\Delta\rho = \rho - \rho_0$ is the difference between the scattering length density of the particle ρ and that of the solvent ρ_0. In the dilute region, the inter-dendrimer interaction can be neglected (i.e., $S(q) \approx 1$), so that the analysis of scattering intensity I(q) can furnish direct information on the form factor P(q), containing information on the dimension of the scattering particles. In the so called (low q) Guinier region (i.e. for $qR_g < 1$), dendrimer form factor can be expressed in terms of the gyration radius (R_g) as $P(q) = P(0)\cdot\exp(-q^2R_g^2/3)$ [28]. Dendrimer gyration radius of R_g has been obtained (see Table 1) from the slope of the representation ln I(q) vs. q^2 as reported in the inset of Fig. 3A and 3B. In Table 1 we also report the dendrimer radius R obtained by the analysis of the sphere form factor $P(q) = [3J_1(qR)/(qR)]^2$ (where $J_1(x) = [\sin(x) - x\cos(x)]/x^2$ is the first-order spherical Bessel function [28].

For a dispersed system of interacting nanoparticles the structure factor S(q), that contains information about the effective inter-particles interaction, can be expressed in terms of the radial pair correlation function g(r) [29,30].

$$S(q) = 1 + \int_0^\infty 4\pi^2\rho_C [g(r) - 1]\frac{\sin(qr)}{(qr)}dr \quad (1)$$

where $\rho_C = c/M$ is the number of particles per unit volume (number density). This equation can be solved numerically by employing different calculation protocols (so called "*closure relations*") in the framework of the Ornstein-Zernike (O.Z.) integral equation and liquid state theory [29–31]. The Ornstein-Zernike approach for the interpretation of the structure factor S(q) has been employed to investigate the strength and range of interparticle interactions in different colloidal systems including amphiphiles micelles, dendrimers, lipid vesicles and proteins [32–35]. In our investigation the repulsive interaction between two dendrimers with a surface charge Ze (where e is the electron charge) and a diameter σ = 2R placed at a distance r has been approximated as (D.L.V.O. potential) [24,36]:

$$U(r) = \frac{Z^2e^2}{4\pi\varepsilon(1 + \kappa\sigma)^2}\frac{e^{-\kappa(r-\sigma)}}{r} \quad (2)$$

where e is the unit of electron charge, ε the dielectric constant and κ is the Debye-Huckel constant, determined, at a given temperature T, by the ionic strength I of the solvent [24].

As shown in Fig. 4A the adopted model for the inter-dendrimers interaction potential (and assuming the hypernetted chain closure relation [30]) reproduces quite satisfactorily SAXS results with an average effective charge of $Z_{eff} = 5.0|e|$ (for G = 2.0) and $Z_{eff} = 12|e|$ (for G = 4.0) for PAMAM dendrimers. It is worth noticing the striking difference in the ionizing ability of the two generations of PAMAM dendrimers in water solution. In fact, only an average number of $Z_{eff} = 12|e|$ amine end-groups over the total $Z_{end} = 64$ end-groups are ionised for G = 4.0 PAMAM dendrimers in water solution. This means that the higher generation G = 4.0 realizes a lower degree of ionization (i.e. $Z_{eff}/Z_{end} = 0.19\%$) in comparison with the lower generation G = 2.0 (i.e. $Z_{eff}/Z_{end} = 0.31\%$) PAMAM dendrimers. This circumstance has its effect also in the expression of the charge at the surface of the DPPC liposome, as evidenced by zeta-potential experiments (Fig. 4B). If we express the ζ-potentials results reported in Fig. 1A in

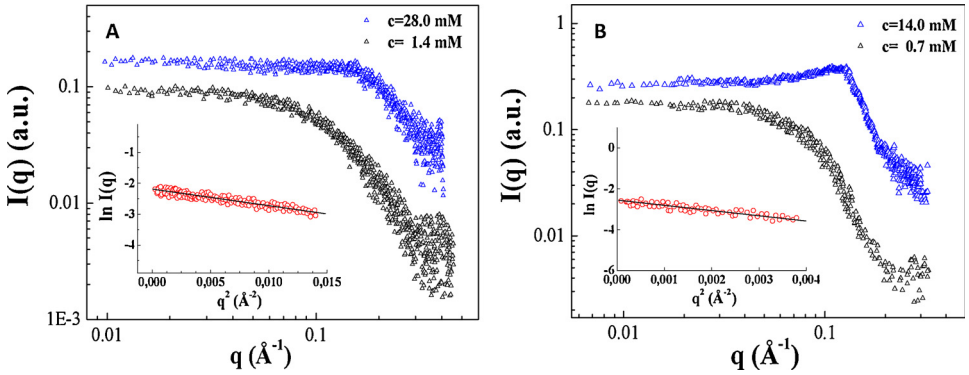

Fig. 3. SAXS profile of water solution of sodium PAMAM dendrimers of generation G = 2.0 (A) and G = 4.0 (B) at different concentrations. In the inset a representation of the Guinier form factor analysis is reported for the systems corresponding to the lower dendrimer concentration.

Table 1
Structural parameters obtained from the small angle x-ray scattering (SAXS) analysis for Poly(amidoamine) dendrimers in water solution (at T = 25 °C).

Generation	M_w (mol/g)	Z_{end} (-NH_2) End-groups	R_g(Å)	R(Å)	Z_{eff} (|e|)
G = 2.0	3256	16	10.6	12.8	5.0
G = 4.0	14,215	64	18.2	23.1	12.0

terms of dendrimer total -NH_2 end-groups/DPPC molar fractions [X_{NH2}/DPPC], we can observe that G = 2.0 PAMAM dendrimers express an higher charge (i.e. ζ–potential) during their inclusion within DPPC vesicles in comparison to G = 4.0 generation (Fig. 4B). This circumstance has been already observed in a recent investigation of model bilayers interacting with generation G = 2.0, 4.0 and 6.0 PAMAM dendrimers [37].

3.3.2. SAXS characterization of the PAMAM/DPPC mixed lipid system

SAXS experiments at different PAMAM/DPPC molar fractions have been performed with the aim to investigate the extent of dendrimer's perturbation in the DPPC bilayer structure. It is worth pointing out that while negligible amounts of multilamellar vesicles (MLVs) are present in extruded lipids of up to 50 nm in liposome diameters, starting from 100 nm liposomes the increase of unilamellar vesicles (ULV) radius results in the presence of more MLVs. This simultaneous presence of multiple (ULVs and MLVs) morphologies, whose presence has been evidenced in different investigations [38–40], often complicates the small angle scattering (SAS) data analysis and interpretation.

In Fig. 5A the influence on DPPC vesicles by inclusion of PAMAM dendrimers of generation G = 2.0 at two different PAMAM/DPPC molar fractions (of X = 0.02 and X = 0.12) are reported. The periodic distances of the DPPC vesicles bilayers (black circles) appear as Bragg reflections in the SAXS pattern, and indicate the presence of multilamellar structures in the system. While a negligible shift in the Bragg-peaks position is detected upon inclusion of G = 2.0 PAMAM dendrimers, a peak broadening (which is more intense at highest dendrimer concentrations X = 0.12) evidences a loss in correlation of the DPPC bilayers (inset of Fig. 5A). Moreover, the inclusion of generation G = 4.0 PAMAM dendrimers exhibits a more perturbing action on DPPC bilayers structure as evidenced in Fig. 5B.

Together with the height decrease (and marked broadening), the Bragg peak q_{max} undergoes a shift toward high q region (inset of Fig. 5A and B) that indicates a change in the characteristic lamellar repeat distance $d = 2\pi h/q_{max}$ (with h = 1, for the 1 st order of the Bragg peak). The fitting with a Lorentz function of the peaks evidenced a lamellar d-spacing which pass from 64 Å (for pure DPPC) to 63 Å (at X = 0.02) and 63 Å (at X = 0.12) in presence of G = 2.0 dendrimers, and to 61 Å (at X = 0.02) and to 61 Å (at X = 0.12) in the presence of G = 4.0 PAMAM dendrimers. Assuming a bilayer thickness for DPPC of 43 Å, those results are compatible with the insertion of G = 4.0 (R_g = 18 Å) and G = 2.0 (R_g = 10 Å) dendrimers between the DPPC

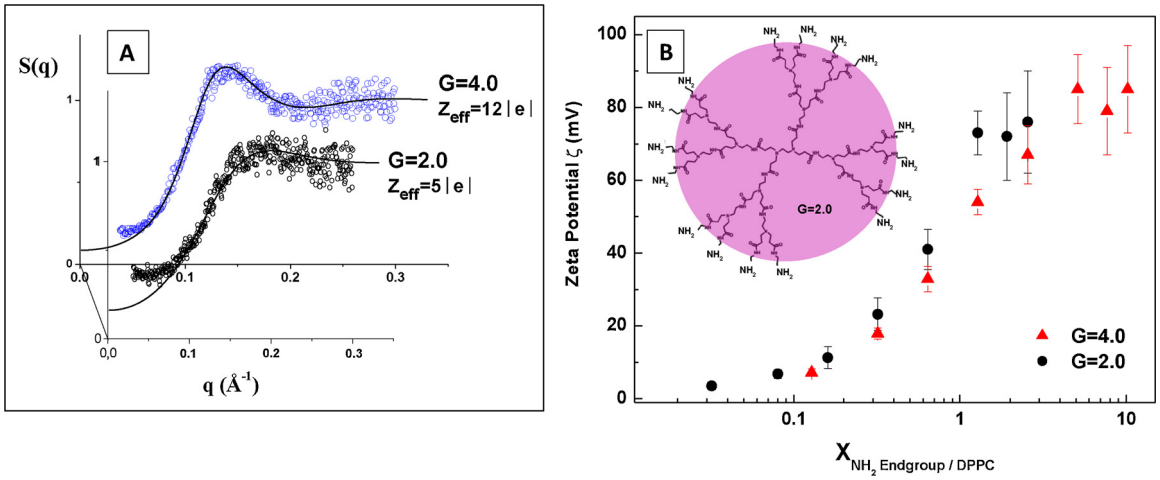

Fig. 4. (A) Analysis of the SAXS structure factor S(q) of the water solution of PAMAM dendrimers, generation G = 2.0 (at c = 0.028 M) and generation G = 4.0 at (at c = 0.014 M). The theoretical calculation (continuous line) is obtained by modelling the D.L.V.O. type inter-dendrimers interaction potential. (B) Zeta potentials (ζ) of the PAMAM/DPPC mixed system in presence of generation G = 2.0 (black circles) and G = 4.0 (red triangles) PAMAM dendrimers. Concentration is expressed in terms of dendrimers total end-groups/DPPC molar fractions ($X_{NH2/DPPC}$).(For interpretation of the references to colour in this figure legend, the reader is referred to the web version of this article.).

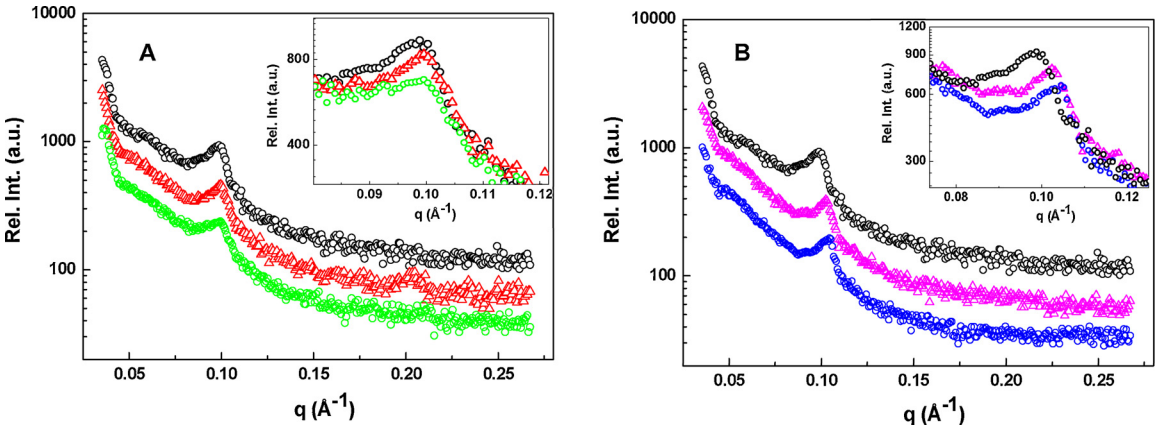

Fig. 5. (A) SAXS spectra of DPPC vesicles alone (black circles) and of the mixed system composed of (G = 2.0) PAMAM/DPPC lipids at the molar fraction of X = 0.02 (red triangles) and X = 0.12 (green circles). In (B) the SAXS spectra of the mixed system composed of (G = 4.0) PAMAM/DPPC lipids at X = 0.02 (pink triangles) and X = 0.12 (blue circles) are also reported.(For interpretation of the references to colour in this figure legend, the reader is referred to the web version of this article.).

bilayers (see Table 1). In this case we can assume that dendrimers fully occupy the space between the bilayers in a bridging mechanism. Such bridging mechanism has been observed in previously investigation by Åkesson et al. [10]

Mixing lipids and dendrimers together in the dry state forces the dendrimers to be incorporated in the lipid bilayer. This favours penetration of dendrimer within the lipid (alkyl chains) hydrophobic region, as evidenced by Raman experiments. The presence of compact structures in the region of lipid-dendrimers interaction has been evidenced also in the case in which dendrimers are successively added in the preformed DPPC vesicles. For example generation G = 7.0 Pamam dendrimers, that are adsorbed on the DPPC bilayer surface, has been shown to act as a bridge between neighbouring lipid vesicles, that leads to flattened lamellar structures and stiffening of the bilayers in the bridging regions [10]. In our specific case, incorporation and penetration of Pamam dendrimers (especially for the higher G = 4.0 generation) could facilitate the bridging 2 neighboring vesicles and the formation of more compact lamellar structures.

On the other hand, the inter-dendrimers electrostatic repulsion may persist over an optimal distance between dendrimers, which is comparable with the Debye-length. In our case we have a Debye-length of $\lambda_D = (\kappa^{-1}) \approx 30$ Å, which is comparable with the diameter ($2R_g$) of the dendrimers. Below this distance, the inter-dendrimers repulsion may limit the adsorption of further dendrimers to the vesicle surface, thus causing a saturation of the vesicle surface with the dendrimers.

Recently, generation G = 5.0 PAMAM dendrimers interacting in the headgroups region of DPPC MLVs evidenced a cooperativity loss of lipid chain packing [41], while the dendrimer binding disrupted the DPPC multilamellar structure with the formation of swollen and fragmented bilayers [41]. Inter-vesicles bridging followed by the formation of larger aggregates or supramolecular complex has been observed in other investigations of mixed dendrimers/lipids systems [7,10]. A recent DSC investigation evidenced also how the incorporation of PAMAM molecules may generate more fluid bilayers structures induced by the weakening of the van der Waals forces between the vesicles alkyl chains [42]. Finally a molecular dynamic (MD) investigation of G = 3.0 PAMAM dendrimers interacting with DMPC bilayers [43] evidenced a nearly spherical dendrimer shape (mainly localized on the bilayer surface) when they interact with gel phase lipids, but a flattened dendrimer configuration (and a significant penetration on the internal alkyl chain region) when interacting with fluid phase lipids.

4. Discussion

Generally, the presence of nanoparticles induces disorder effects in the structure of the lipid bilayers, while the final morphology is strongly determined by the size, charge and composition of the interacting components [44–48]. As an example, it has been shown that inclusion of bile salts induces a structural perturbation against the long-range cohesive tendency of the lipid bilayers vesicles [49–51]. Its inclusion favors, in fact, fragmentation of initial lipid bilayer structure in variety of complementary morphologies. Those processes play a crucial role in nutrients absorption during digestion process [51–53].

The findings of our study evidence that PAMAM dendrimer interacts with DPPC lipid molecules both at the liposomes surface and in the hydrophobic region of the lipids bilayers. Moreover, the inclusion of charged dendrimers causes a linear increase of the zeta potential (i.e. an increase of the liposome surface charge) with increasing PAMAM concentration up to a fixed concentration (namely, $X_{G4} = 0.04$ for the G = 4.0 and $X_{G2} = 0.08$ for the G = 2.0 dendrimer's generation). It is worth pointing that, for higher dendrimer concentrations outside the linear region, we also observed an increase in the liposome hydrodynamic radius (see Fig. 1B). This circumstance may be explained assuming that the perturbation of the alkyl chain (order/disorder transition with liquidation of the compact hydrophobic region of the bilayer), is followed by a structural reorganization of the liposomes.

Interestingly, the linear region extends toward higher concentrations as the dendrimer generation decreases from G = 4.0 to G = 2.0 (see Fig. 1B). In this case, the higher PAMAM concentration (limit molar fraction X) within the liner interval allows us to calculate the number of DPPC lipids N_{DPPC} (per single PAMAM dendrimer) that are necessary to ensure a stable liposome structure (characterized by a liposome hydrodynamic radius close to the extrusion dimension, R = 50 nm). This parameter, N_{DPPC}, grows linearly with the dendrimer molecular weight (M_w) as evidenced in Fig. 6.

Moreover, if we compare the surface covered by each dendrimer (estimated as $S_D = \pi R_g^2$) with the surface of the corresponding surrounding lipids N_{DPPC} (Fig. 6), we obtain that about 58% of vesicle surface is covered in presence of G = 4.0 dendrimers (and about 38% in presence of the G = 2.0 dendrimers). This circumstance implies that G = 4.0 Pamam dendrimers perturb the DPPC vesicles structure much more than G = 2.0, thus confirming previous results.

A relevant aspect of the employment of dendrimers in bio-nanotechnology is connected with their electrostatic interaction, as the charge plays a crucial role as control parameter in many smart application in nano-technology as well as in various approaches for the synthesis of nanostructures (directed by dendrimer's charge) [54–57].

In our study, the observation of a linear increase of the liposome ζ-potential indicates the direct involvement of the positive dendrimer charges in the expression of the DPPC vesicles electrostatic potential. If we limit our analysis to the linear region of the ζ-potential (ζ < 100 mV), we can estimate the charge density σ at the surface of the

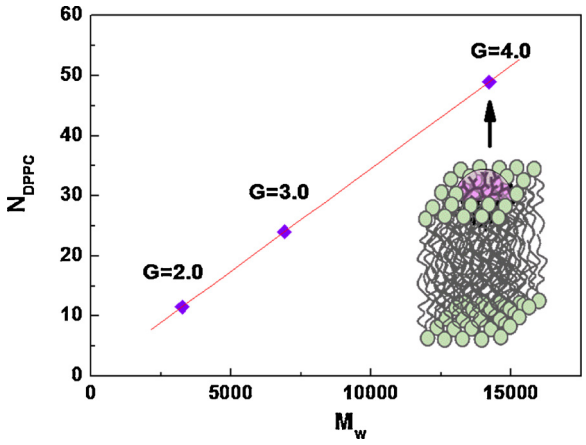

Fig. 6. Number of DPPC lipids N_{DPPC} (per single PAMAM dendrimer) corresponding to the upper limit concentration X, within the liner region of the Zeta-potential (Fig. 1A). The result for PAMAM dendrimers of generation G = 3.0 is calculated from data of ref. [11].

mixed PAMAM/DPPC vesicles system through the equation [24,58]

$$\sigma = \sqrt{8n\varepsilon_0\varepsilon_r k_B T}\cdot\frac{e\zeta}{2k_B T} = \frac{\varepsilon_0\varepsilon}{\kappa^{-1}}\zeta \quad (3)$$

Where n is the bulk solution concentration and $\kappa^{-1}=\lambda_D$ is the Debye screening length, corresponding to the inverse of the Debye-Huckel constant[24]. From the liposome charge density σ we can calculate the total charge $Z_{VES}= \sigma\cdot(4\pi R_V^2)$ at the surface of the DPPC vesicles of radius R_V, as reported in the inset of Fig. 7A. Finally, by dividing the effective vesicles charge Z_{VES} by the number of dendrimers N_D in each vesicle we can estimate of the effective charge expressed by each dendrimer at the surface of the liposome, as reported in Fig. 7A (see [Appendix A]).

As reported in Fig. 7 the average (individual) dendrimer charge of Z^*_{eff} = 0.52 (for G = 2.0) and Z^*_{eff} = 1.50 (for G = 4.0) results considerably attenuated if compared with the dendrimer effective charges of Z_{eff} = 5.0 (for G = 2.0) and Z_{eff} = 12.0 (for G = 4.0) previously obtained by means of the SAXS analysis structure factor S(q) in the framework of the D.L.V.O. approach (see Section 3.1). The difference in the detected dendrimer charge can be explained assuming that dendrimers are embedded (more or less deeply) within the bilayer hydrophobic region (Fig. 7B).

Our result evidences also that outside the linear region of the ζ-potential, further increase in the amount of dendrimers does not cause a proportional expression of charges in the surface of the liposomes, as dendrimer inclusion probably promotes the formation of more complex morphology with region of high dendrimer concentration in the internal portions of the bilayers. In this respect the possible structural reorganization may promote disruptive effect of the dendrimers during their interaction with bio-membranes that may be associated with unwanted effects [8,20].

Employment of suitable modelling approaches in conjunction with different techniques is crucial to understand the key properties mechanisms underlying the complex phenomena present during self-association processes in lipid bio-membranes under various conditions [59–63], and provides important indication about the key features of cytotoxicity effects in cellular membranes, suitable for advanced applications in biotechnology and nanomedicine.

5. Conclusion

The interaction of PAMAM dendrimers (generation G = 2.0 and G = 4.0) with DPPC lipids was investigated by using combined ζ-potential, Raman spectroscopy and small angle x-ray scattering (SAXS) measurements on extruded vesicles at different dendrimer concentration. Obtained results highlighted a significant interaction between PAMAM dendrimers and DPPC molecules both in the internal region of the bilayers as well as in the surface of the liposome. Analysis of the SAXS structure factor with a suitable model for the inter-dendrimers electrostatic potential allows an estimation of the dendrimer effective charge, while only a fraction of this charge contributes to the linear increase of liposome zeta-potential. Outside the linear region of the ζ-potential, further increase in dendrimer concentration favors a reduction in the cooperativity of the alkyl chains followed by a loss in multilamellar correlation and an alteration/reorganization of the structure characterized by the increase in the liposome hydrodynamic radius. This study highlights some critical issues connected with possible disruptive effect of polymer–based (soft) nanoparticles during the interaction with biological membranes and that may be associated with unwanted cytotoxicity effects of the nanoparticles inclusion process.

Acknowledgments

D.L. acknowledges funding from Marie Curie Actions under EU FP7 Initial Training Network SNAL 608184. The work of M.A.K. was financed by the Russian Scientific Foundation (Project no. 14-12-00516).

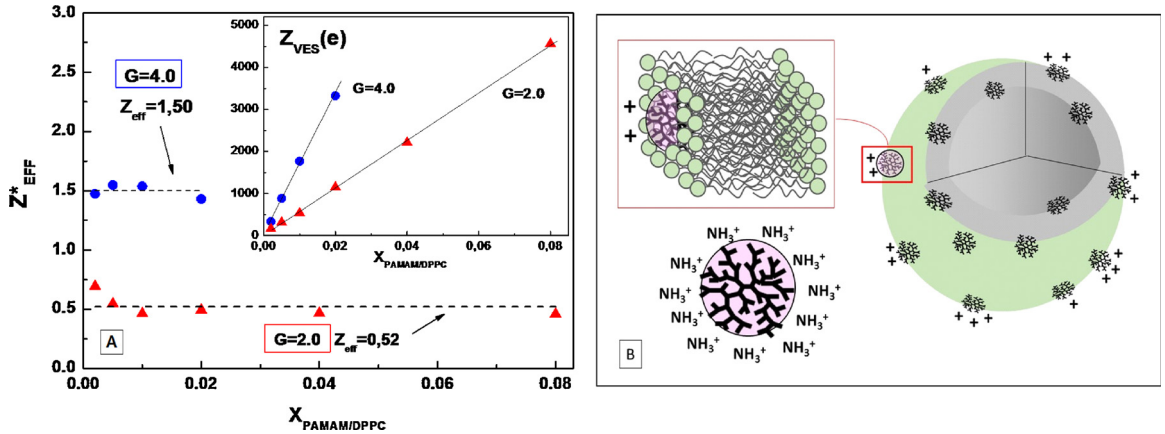

Fig. 7. Average charge (in unit of electron charge |e|) expressed by individual dendrimers at the surface of the liposome (A). Effective vesicle charge Z_{VES} at different PAMAM/DPPC molar rations X (inset in panel A). Effective dendrimer charge expressed at the surface of the liposome during inclusion in DPPC vesicles (B).

Appendix A

The vesicles effective charge Z_{VES} is an important parameter in order to assess the dendrimer concentration effect on the structural properties of DPPC vesicle in solution. We can express the total surface area of a spherical DPPC bilayer vesicle A_{Ves} as the sum of the outer (A_{out}) plus inner (A_{in}) surface area:

$$A_{Ves} = A_{out} + A_{in} = 4\pi R_V^2 + 4\pi (R_V - d_{DPPC})^2 \quad \text{(A1)}$$

where $d_{DPPC} = 4.9$ nm is the average value of bilayer thickness obtained for a gel-phase of a DPPC lipid) [64–66] and $R_v = 50$ nm is the average vesicle radius (corresponding to the extrusion process). From the knowledge of the average area per DPPC lipid molecule (within a lipid bilayer) [64–66] $A_{DPPC} = 0.50\,nm^2$ we can calculate the average number of lipid molecules in each vesicle as $N_{Lip} = A_{Ves}/A_{DPPC}$. Finally, the number of dendrimers N_D in each vesicle (for each molar fraction X) can be obtained by the following relation.

$$N_D = \frac{X}{1 - X} N_{Lip} \quad \text{(A2)}$$

By dividing the vesicles effective charge Z_{VES} (inset of Fig. 7A) by the corresponding number of dendrimers in each vesicle N_D, we can obtain the effective charge expressed by each dendrimer at the surface of the liposome (Fig. 7A).

References

[1] S. Svenson, D.A. Tomalia, Dendrimers in biomedical applications - reflections on the field, Adv. Drug Deliv. Rev. 64 (2012) 102–115.
[2] R.M. Kannan, E. Nance, S. Kannan, D.A. Tomalia, Emerging concepts in dendrimer-based nanomedicine: from design principles to clinical applications, J. Intern. Med. 276 (2014) 579–617.
[3] L.-P. Wu, M. Ficker, J.B. Christensen, P.N. Trohopoulos, S.M. Moghimi, Dendrimers in medicine: therapeutic concepts and pharmaceutical challenges, Bioconjug. Chem. 26 (2015) 1198–1211.
[4] J. Singh, K. Jain, N.K. Mehra, N.K. Jain, Dendrimers in anticancer drug delivery: mechanism of interaction of drug and dendrimers, Artif. Cells Nanomed. Biotechnol. 44 (2016) 1626–1634.
[5] C.N. Likos, M. Schmidt, H. Löwen, M. Ballauff, D. Pötschke, P. Lindner, Soft interaction between dissolved flexible dendrimers: theory and experiment, Macromolecules 34 (2001) 2914–2920.
[6] D. Lombardo, Modeling dendrimers charge interaction in solution: relevance in biosystems, Biochem. Res. Int. (2014) 1–10 837651.
[7] C.V. Kelly, M.G. Liroff, L.D. Triplett, P.R. Leroueil, D.G. Mullen, J.M. Wallace, S. Meshinchi, J.R. Baker Jr., B.G. Orr, M.M. Banaszak Holl, Stoichiometry and structure of poly(amidoamine) dendrimer-lipid complexes, ACS Nano 3 (2009) 1886–1896.
[8] S. Parimi, T.J. Barnes, D.F. Callen, C.A. Prestidge, Mechanistic insight into cell growth, internalization, and cytotoxicity of PAMAM dendrimers, Biomacromolecules 11 (2010) 382–389.
[9] Z.Y. Zhang, B.D. Smith, High-generation polycationic dendrimers are unusually effective at disrupting anionic vesicles: membrane bending model, Bioconjug. Chem. 11 (2000) 805–814.
[10] A. Åkesson, K.M. Bendtsen, M.A. Beherens, J.S. Pedersen, V. Alfredsson, M.C. Gomez, The effect of PAMAM G6 dendrimers on the structure of lipid vesicles, Phys. Chem. Chem. Phys. 12 (2010) 12267–12272.
[11] D. Lombardo, P. Calandra, E. Bellocco, G. Laganà, D. Barreca, S. Magazù, U. Wanderlingh, M.A. Kiselev, Effect of anionic and cationic polyamidoamine (PAMAM) dendrimers on a model lipid membrane, BBA Biomembranes 1858 (2016) 2769–2777.
[12] K. Gardikis, S. Hatziantoniou, M. Signorelli, M. Pusceddu, M. Micha-Screttas, A. Schiraldi, C. Demetzos, D. Fessas, Thermodynamic and structural characterization of liposomal-locked in-dendrimers as drug carriers, Colloids Surf. B 81 (2010) 11–19.
[13] D. Lombardo, P. Calandra, D. Barreca, S. Magazù, M.A. Kiselev, Soft interaction in liposome nanocarriers for therapeutic drug delivery, Nanomaterials 6 (2016) 125.
[14] M. Wilde, R.J. Green, M.R. Sanders, F. Greco, Biophysical studies in polymer therapeutics: the interactions of anionic and cationic PAMAM dendrimers with lipid monolayers, J. Drug Target. 25 (2017) 910–918.
[15] J. Matraszek, E. Gorecka, J. Mieczkowski, M. Hejko, D. Pociecha, Hierarchical structures formed by flexible dendrimeric molecules based on gallic acid, Macromol. Chem. Phys. 1700316 (1-5) (2017).
[16] C.J. Morris, G. Aljayyoussi, O. Mansour, P. Griffiths, M. Gumbleton, Endocytic uptake, transport and macromolecular interactions of anionic PAMAM dendrimers within lung tissue, Pharm. Res. 34 (2017) 2517–2531, http://dx.doi.org/10.1007/s11095-017-2190-7.
[17] A. Mazzaglia, A. Scala, G. Sortino, R. Zagami, Y. Zhu, M.T. Sciortino, R. Pennisi, M.M. Pizzo, G. Neri, G. Grassi, A. Piperno, Intracellular trafficking and therapeutic outcome of multiwalled carbon nanotubes modified with cyclodextrins and polyethylenimine, Colloids Surf. B Biointerfaces 163 (2018) 55–63.
[18] C. Ceresa, G. Nicolini, R. Rigolio, M. Bossi, L. Pasqua, G. Cavaletti, Functionalized mesoporous silica nanoparticles: a possible strategy to target cancer cells reducing peripheral nervous system uptake, Curr. Med. Chem. 20 (2013) 2589–2600.
[19] N. Dan, Nanostructured lipid carriers: effect of solid phase fraction and distribution on the release of encapsulated materials, Langmuir 30 (2014) 13809–13814.
[20] T.P. Thomas, I. Majoros, A. Kotlyar, D. Mullen, M.M. Banaszak Holl, J.R. Baker Jr., Cationic poly(amidoamine) dendrimer induces lysosomal apoptotic pathway at therapeutically relevant concentrations, Biomacromolecules 10 (2009) 3207–3214.
[21] M. Kluzek, A.I.I. Tyler, S. Wang, R. Chen, C.M. Marques, F. Thalmann, J.M. Seddon, M. Schmutz, Influence of a pH-sensitive polymer on the structure of monoolein cubosomes, Soft Matter 13 (2017) 7571–7577.
[22] S. Ramadurai, M. Werner, N.K.H. Slater, A. Martin, V.A. Baulin, T.E. Keyes, Dynamic studies of the interaction of a pH responsive, amphiphilic polymer with a DOPC lipid membrane, Soft Matter 13 (2017) 3690–3700.
[23] F. McNeil-Watson, W. Tscharnuter, J. Miller, A new instrument for the measurement of very small electrophoretic mobilities using phase analysis light scattering (PALS), Colloids Surf. A Physicochem. Eng. Asp. 140 (1998) 53–57.
[24] R.J. Hunter, Foundations of Colloid Science vols. I−II, Oxford University Press, NewYork, 1986.
[25] B.J. Berne, R. Pecora, Dynamic Light Scattering, John Wiley, New York, 1976.
[26] C. Huang, I.W. Levin, Effect of lipid chain length inequivalence on the packing characteristics of bilayer assemblies. Raman spectroscopy study of phospholipid dispersion in the gel state, J. Phys. Chem. 87 (1983) 1509–1513.
[27] N.B. Colthulp, L.H. Daly, S.E. Wiberley, Introduction to Infrared and Raman Spectroscopy, Academic Press, New York, 1990.
[28] O. Glatter, O. Kratky, Small-Angle X-Ray Scattering, Academic Press, London, 1982.
[29] J.P. Hansen, I.A. Mc Donald, Theory of Simple Liquids, Academic Press, New-York, 1986.
[30] L. Belloni, Interacting monodisperse and polydisperse spheres, in: P. Lindner, T. Zemb (Eds.), Neutron X-Ray and Light Scattering, Elsevier Science Publishers B.V., New York, 1991.
[31] J.B. Hayter, J. Penfold, An analytic structure factor for macroion solutions, Mol. Phys. 42 (1981) 109–118.
[32] L. Cantù, M. Corti, T. Zemb, C. Williams, Small angle X-ray and neutron scattering from ganglioside micellar solutions, J. Phys.-Paris 03 (C8) (1993) 221–227.
[33] N. Micali, L.M. Scolaro, A. Romeo, D. Lombardo, P. Lesieur, F. Mallamace, Structural properties of methanol-polyamidoamine dendrimer solutions, Phys. Rev. E 58 (1998) 6229–6235.
[34] C.A. Faunce, H.H. Paradies, Observations of liquidlike order of charged rodlike lipid a diphosphate assemblies at pH 8.5, J. Chem. Phys. 128 (1–8) (2008) 065105.
[35] M.C. Abramo, C. Caccamo, D. Costa, G. Pellicane, R. Ruberto, U. Wanderlingh, Effective interactions in lysozyme aqueous solutions: a small-angle neutron scattering and computer simulation study, J. Chem. Phys. 136 (2012) 035103.
[36] E.J.W. Verwey, J.Th.G. Overbeek, Theory of the Stability of Lyophobic Colloids, Elsevier, Amsterdam, 1948.
[37] B. Roy, A.K. Panda, S. Parimi, I. Ametov, T. Barnes, C.A. Prestidge, Physico-chemical studies on the interaction of dendrimers with lipid bilayers. 1. Effect of dendrimer generation and liposome surface charge, J. Oleo Sci. 63 (2014) 1185–1193.
[38] H. Schmiedel, L. Almásy, G. Klose, Multilamellarity, Structure and hydration of extruded POPC vesicles by SANS, Eur. Biophys. J. 35 (2006) 181–189.
[39] N. Kucerka, J. Pencer, J.N. Sachs, J.F. Nagle, J. Katsaras, Curvature effect on the structure of phospholipid bilayers, Langmuir 23 (2007) 1292–1299.
[40] P. Calandra, D. Caschera, V.T. Liveri, D. Lombardo, How self-assembly of amphiphilic molecules can generate complexity in the nanoscale, Colloids Surf. A Physicochem. Eng. Asp 484 (2015) 164–183.
[41] S. Berényi, J. Mihály, A. Wacha, O. Tőke, A. Bóta, A mechanistic view of lipid membrane disrupting effect of PAMAM dendrimers, Colloids Surf. B Biointerfaces 118 (2014) 164–171.
[42] K. Gardikis, S. Hatziantoniou, K. Viras, M. Wagner, C. Demetzos, A DSC and raman spectroscopy study on the effect of PAMAM dendrimer on DPPC model lipid membranes, Int. J. Pharm. 318 (2006) 118–123.
[43] C.V. Kelly, P.R. Leroueil, B.G. Orr, M.M. Banaszak Holl, I. Andricioaei, Poly(amidoamine) dendrimers on lipid bilayers II: effects of bilayer phase and dendrimer termination, J. Phys. Chem. B 112 (2008) 9346–9353.
[44] J.P. Prates Ramalho, P. Gkeka, L. Sarkisov, Structure and phase transformations of DPPC lipid bilayers in the presence of nanoparticles: insights from coarse-grained molecular dynamics simulations, Langmuir 27 (2011) 3723–3730.
[45] M. Ionov, K. Gardikis, D. Wróbel, S. Hatziantoniou, H. Mourelatou, J.-P. Majoral,

B. Klajnert, M. Bryszewska, C. Demetzos, Interaction of cationic phosphorus dendrimers (CPD) with charged and neutral lipid membranes, Colloids Surf. B Biointerfaces 82 (2011) 8–12.
[46] M. Schulz, A. Olubummo, W.H. Binder, Beyond the lipid-bilayer: interaction of polymers and nanoparticles with membranes, Soft Matter 8 (2012) 4849–4864.
[47] Y. Yang, S. Sunoqrot, C. Stowell, J. Ji, C.-W. Lee, J.W. Kim, S.A. Khan, S. Hong, Effect of size, surface charge, and hydrophobicity of poly(amidoamine) dendrimers on their skin penetration, Biomacromolecules 13 (2012) 2154–2162.
[48] C. Conte, A. Scala, G. Siracusano, G. Sortino, R. Pennisi, A. Piperno, A. Miro, F. Ungaro, M.T. Sciortino, F. Quaglia, A. Mazzaglia, Nanoassemblies based on non-ionic amphiphilic cyclodextrin hosting Zn(II)-phthalocyanine and docetaxel: design, physicochemical properties and intracellular effects, Colloids Surf. B Biointerfaces 146 (2016) 590–597.
[49] M. Ollivon, S. Lesieur, C. Grabielle-Madelmont, M. Paternostre, Vesicle reconstitution from lipid–detergent mixed micelles, BBA Biomembranes 1508 (2000) 34–50.
[50] M.A. Kiselev, D. Lombardo, P. Lesieur, A.M. Kisselev, S. Borbely, T.N. Simonova, L.I. Barsukov, Membrane self assembly in mixed DMPC/NaC systems by SANS, Chem. Phys. 345 (2008) 173–180.
[51] M.M. Elsayeda, G. Cevc, The vesicle-to-micelle transformation of phospholipid–cholate mixed aggregates: a state of the art analysis including membrane curvature effects, BBA Biomembranes 1808 (2011) 140–153.
[52] J. Maldonado-Valderrama, P. Wilde, A. Macierzanka, A. Mackie, The role of bile salts in digestion, Adv. Colloid Interface Sci. 165 (2011) 36–46.
[53] M.A. Kiselev, M. Janich, A. Hildebrand, P. Strunz, R.H.H. Neubert, D. Lombardo, Structural transition in aqueous lipid/bile salt [DPPC/NaDC] supramolecular aggregates: SANS and DLS study, Chem. Phys. 424 (2013) 93–99.
[54] W.-D. Jang, D.-L. Jiang, T. Aida, Dendritic physical gel: hierarchical self-organization of a peptide-core dendrimer to form a micrometer-scale fibrous assembly, J. Am. Chem. Soc. 122 (2000) 3232–3233.
[55] L. Bonaccorsi, D. Lombardo, A. Longo, E. Proverbio, A. Triolo, Dendrimer template directed self-assembly during zeolite formation, Macromolecules 42 (2009) 1239–1243.
[56] K. Sato, J. Anzai, Dendrimers in layer-by-layer assemblies: synthesis and applications, Molecules 18 (2013) 8440–8460.
[57] P. Kesharwani, K. Jain, N.K. Jain, Dendrimer as nanocarrier for drug delivery, Prog. Polym. Sci. 39 (2014) 268–307.
[58] D.C. Graham, The electrical double layer and the theory of electrocapillarity, Chem. Rev. 41 (1947) 441–501.
[59] M. Breton, J.-F. Berret, C. Bourgaux, T. Kral, M. Hof, C. Pichon, M. Bessodes, D. Scherman, N. Mignet, Protonation of lipids impacts the supramolecular and biological properties of their self-assembly, Langmuir 27 (2011) 12336–12345.
[60] A. Weinberger, V. Walter, S.R. MacEwan, T. Schmatko, P. Muller, A.P. Schroder, A. Chilkoti, C.M. Marques, Cargo self-assembly rescues affinity of cell-penetrating peptides to lipid membranes, Sci. Rep. 7 (2017) 43963.
[61] C. Bourgaux, P. Couvreur, Interactions of anticancer drugs with biomembranes: what can we learn from model membranes? J. Control. Release 190 (2014) 127–138.
[62] A. Åkesson, C.V. Lundgaard, N. Ehrlich, T.G. Pomorski, D. Stamou, M. Cárdenas, Induced dye leakage by PAMAM G6 does not imply dendrimer entry into vesicle lumen, Soft Matter 8 (2012) 8972–8980.
[63] F. Ruggeri, A. Akesson, P.-Y. Chapuis, C.A. Skrzynski Nielsen, M.P. Monopoli, K.A. Dawson, T.G. Pomorski, M. Cardenas, The dendrimer impact on vesicles can be tuned based on the lipid bilayer charge and the presence of albumin, Soft Matter 9 (2013) 8862–8870.
[64] M.C. Wiener, R.M. Suter, J.F. Nagle, Structure of the fully hydrated gel phase of dipalmitoylphosphatidylcholine, Biophys. J. 55 (1989) 315–325.
[65] J.F. Nagle, S. Tristram-Nagle, Structure of lipid bilayers, Biochim. Biophys. Acta 1469 (3) (2000) 159–195.
[66] M.A. Kiselev, D. Lombardo, Structural characterization in mixed lipid membrane systems by neutron and X-ray scattering, BBA Gen. Subj. 1861 (2017) 3700–3717.